NeuroImage: Clinical 7 (2015) 755–763

Contents lists available at ScienceDirect

NeuroImage: Clinical

journal homepage: www.elsevier.com/locate/ynicl

Co-localization between the BOLD response and epileptiform discharges recorded by simultaneous intracranial EEG-fMRI at 3 T

Yahya Aghakhani[a], Craig A. Beers[a,b,c], Daniel J. Pittman[a,b,c], Ismael Gaxiola-Valdez[a,b,c], Bradley G. Goodyear[a,b,c,d,e], Paolo Federico[a,b,c,e,*]

[a]Department of Clinical Neurosciences, University of Calgary
[b]Hotchkiss Brain Institute, University of Calgary, Canada
[c]Seaman Family MR Research Centre, University of Calgary, Canada
[d]Department of Psychiatry, University of Calgary, Canada
[e]Department of Radiology, University of Calgary, Canada

ARTICLE INFO

Available online 7 March 2015

Keywords:
EEG-fMRI
intracranial EEG
Epileptiform discharge
BOLD response

ABSTRACT

Objectives: Simultaneous scalp EEG-fMRI can identify hemodynamic changes associated with the generation of interictal epileptiform discharges (IEDs), and it has the potential of becoming a standard, non-invasive technique for pre-surgical assessment of patients with medically intractable epilepsy. This study was designed to assess the BOLD response to focal IEDs recorded via simultaneous intracranial EEG-functional MRI (iEEG-fMRI).
Methods: Twelve consecutive patients undergoing intracranial video EEG monitoring were recruited for iEEG-fMRI studies at 3 T. Depth, subdural strip, or grid electrodes were implanted according to our standard clinical protocol. Subjects underwent 10–60 min of continuous iEEG-fMRI scanning. IEDs were marked, and the most statistically significant clusters of BOLD signal were identified (Z-score 2.3, p value < 0.05). We assessed the concordance between the locations of the BOLD response and the IED. Concordance was defined as a distance <1.0 cm between the IED and BOLD response location. Negative BOLD responses were not studied in this project.
Results: Nine patients (7 females) with a mean age of 31 years (range 22–56) had 11 different types of IEDs during fMR scanning. The IEDs were divided based on the location of the active electrode contact into mesial temporal, lateral temporal, and extra-temporal. Seven (5 left) mesial temporal IED types were recorded in 5 patients (110–2092 IEDs per spike location). Six of these IEDs had concordant BOLD response in the ipsilateral mesial temporal structures, <1 cm from the most active contact. One of the two subjects with left lateral temporal IEDs had BOLD responses concordant with the location of the most active contact, as well other ipsilateral and contralateral sites. Notably, the remaining two subjects with extratemporal discharges showed no BOLD signal near the active electrode contact.
Conclusions: iEEG-fMRI is a feasible and low-risk method for assessment of hemodynamic changes of very focal IEDs that may not be recorded by scalp EEG. A high concordance rate between the location of the BOLD response and IEDs was seen for mesial temporal (6/7) IEDs. Significant BOLD activation was also seen in areas distant from the active electrode and these sites exhibited maximal BOLD activation in the majority of cases. This implies that iEEG-fMRI may further describe the areas involved in the generation of IEDs beyond the vicinity of the electrode(s).

1. Introduction

Scalp electroencephalography (EEG) is widely regarded as an effective method for recording epileptic discharges, and is a mainstay in a typical epilepsy unit. Despite its widespread use, however, there are inherent limitations. Scalp EEG primarily records activity of pyramidal neurons near the surface of the brain. Thus, epileptiform activity originating from deep sources is not recorded. In addition, a minimum of 10–20 cm^2 of synchronous, or nearly synchronous activity is required for the detection of interictal epileptiform discharges (IEDs) with scalp EEG (Tao et al., 2005). Hence, IEDs originating from small regions of epileptogenic cortex are not recorded. Finally, the spatial resolution of scalp EEG is only 22–37 cm^3 when

Abbreviations: IED, interictal epileptiform discharge; VEM, video-EEG monitoring.

* Corresponding author at: Hotchkiss Brain Institute, University of Calgary, Foothills Medical Centre, Room C1214a, 1403 29th Street NW, Calgary, AB T2N 2T9, Canada. Tel.: +1 403 944 4091; fax: +1 403 283 2270.
E-mail address: pfederic@ucalgary.ca (P. Federico).

http://dx.doi.org/10.1016/j.nicl.2015.03.002

using a routine set of 19 electrodes, and improves to only 6–8 cm^3 when using up to 128 electrodes (Ferree et al., 2001).

The poor spatial resolution of scalp EEG can be mitigated by combining EEG with functional magnetic resonance imaging (fMRI). Simultaneous EEG-fMRI can also noninvasively evaluate the hemodynamic changes associated with IEDs and has been used successfully for presurgical assessment of patients with medically intractable epilepsy (An et al., 2013; Gotman and Pittau, 2011; Laufs and Duncan, 2007; Moeller et al., 2009; Thornton et al., 2010; Zijlmans et al., 2007). For example, an EEG-fMRI study of 29 patients initially rejected for epilepsy surgery due to inaccurate localization of the seizure focus through standard clinical investigations, identified focal and significant blood oxygen level dependent (BOLD) responses in 15 subjects (Zijlmans et al., 2007). Eight of these 15 subjects had a BOLD response concordant with IED localization. Furthermore, two patients subsequently underwent intracranial EEG (iEEG) monitoring; the BOLD response showed concordance with the ictal onset zone determined by iEEG. One of these patients underwent surgical resection and had a good post-surgical outcome (Engel class II). In another EEG-fMRI study, the BOLD signal from nine non-lesional frontal lobe epilepsy patients was compared to the topography of spikes, and to positron emission tomography and single photon emission computerized tomography results, when available (Moeller et al., 2009). Concordance between IED localization and the location of BOLD response was demonstrated in 8 of the 9 patients. In two cases, reviewing the structural MRI guided by EEG-fMRI data resulted in the consideration of a suspicious, deep sulcus as potential pathology. These two patients subsequently underwent surgical resection and histology confirmed cortical dysplasia in one and microdysgenesis in the other. The EEG-fMRI data had shown activation just adjacent to the resected pathologic area. These studies suggest that scalp EEG-fMRI provides added value as a pre-surgical tool; however, the limitations of scalp EEG's insensitivity to deep structures and to small regions of epileptogenic cortex remain.

Compared to scalp EEG, iEEG has greater sensitivity and spatial specificity for recording focal IEDs from deep structures such as the mesial temporal regions (Morris and Luders, 1985), and the area of cortex required for detection using iEEG is reduced to within a 1 cm vicinity of the recording electrode (Lachaux et al., 2003). In combination with fMRI, iEEG thus possesses great clinical potential. With this in mind, our research group recently assessed the risk and feasibility of simultaneous iEEG-fMRI at 3 T in phantoms and epilepsy patients (Boucousis et al., 2012; Cunningham et al., 2012). We found that standard gradient-echo based structural and functional MR protocols did not induce any clinically significant electrode heating, electrode movement, or electrical currents. As such, simultaneous iEEG-fMRI was deemed low-risk by our local ethics and safety committee. Since then, we have been actively using simultaneous iEEG-fMRI for the study of epilepsy patients. In the present study, we assessed the concordance between the location of focal IEDs and the associated BOLD responses recorded with simultaneous iEEG-fMRI.

2. Methods

2.1. Intracranial EEG subjects

The Conjoint Health Research Ethics Board of our institution approved this project. Written informed consent was obtained from all participants prior to their participation. Twelve consecutive patients undergoing intracranial video-EEG monitoring (VEM) at our center were recruited. The inclusion criteria included: age ≥ 18 years, no MR contraindications (e.g., ferromagnetic implants, claustrophobia), no post-implantation complications (e.g., subdural hematoma, infection, severe headache), and the ability to provide informed consent.

Intracranial VEM data were reviewed by an experienced epileptologist (PF) to select electrodes for recording during the iEEG-fMRI session. The first seven subjects had the two most active strip or depth electrodes selected for data collection. Electrodes were attached via commercially available connector blocks (product number L-SRL-10DIN; Ad-Tech, Racine, WI) to a custom-built, two-tailed electrode connector capable of recording 19 contacts (Compumedics NeuroScan, Charlotte, NC) and coupled with a commercial scalp EEG-fMRI system (MagLink RT; Compumedics NeuroScan). The next five subjects had up to eight strip or depth electrodes selected for data collection. These electrodes were attached to a custom built, eight-tailed electrode connector capable of recording 64 contacts (Compumedics NeuroScan). We have previously shown that these connectors are of low-risk in our 3 Tesla environment (Boucousis et al., 2012; Cunningham et al., 2012).

2.2. iEEG-fMRI acquisition

The subjects underwent 10–60 min of fMRI scanning as per the gradual implementation protocol established prior to the start of the project (see Cunningham et al., 2012). EEG data were continuously collected at 10 kHz using a SynAmps^2 amplification/digitization system and Scan 4.4 Software (Compumedics NeuroScan). The first seven subjects were scanned using a 3 Tesla GE, Signa LX whole body scanner and a receive-only eight-channel phased-array head coil, while the last five subjects were scanned using a 3 Tesla GE Discovery MR750 whole body scanner and a receive-only eight-channel phased-array coil (GE Healthcare, Waukesha, WI). No adverse events were reported during the scanning of any patient.

The MR imaging protocol for the 3.0 T GE, Signa LX scanner included multislice anatomical imaging (spoiled gradient-recalled echo, TE = min full, TR = 150 ms, flip angle = 18°, 128 × 128 matrix, 24 5-mm thick slices), anatomical 3D T_1-weighted imaging (magnetization-prepared rapid gradient-echo: TE = min full, TR = 8.9 ms, flip angle = 20°, 384 × 256 × 64 matrix, 2-mm thick slices), a non-linear shimming sequence to minimize magnetic field inhomogeneities, and fMRI (gradient recalled echo planar imaging sequence, with TE = 30 ms, TR = 1500 ms, flip angle = 60°, 24-cm field of view, 64 × 64 matrix, 24 5-mm thick slices). The MR imaging protocol for the 3.0 T GE Discovery MR750 included multislice anatomical imaging (spoiled gradient-recalled echo 2D multi-slice sequence, TE = 2.1 ms, TR = 150 ms, flip angle = 18°, 128 × 128 matrix, 24 5-mm thick slices), anatomical 3D T_1-weighted imaging (TE = 3.8 ms, TR = 9.3 ms, flip angle = 12°, 24-cm field of view, 320 × 256 × 64 matrix, 2-mm thick slices), a non-linear shimming sequence to minimize magnetic field inhomogeneities, and fMRI (spoiled gradient recalled echo planar imaging, TE = 30 ms, TR = 1500 ms, flip angle = 65°, 24-cm field of view, 64 × 64 matrix, 24 5-mm thick slices).

The subjects' heads were immobilized in the head coil using compressible foam cushions, and the electrode tails/connector blocks were directed outside of the coil, padded, and secured to the scanning table to minimize movement, vibration, and RF energy deposition. Subjects were encouraged to sleep. During iEEG-fMRI data collection, EEG recordings were filtered online for viewing purposes and were monitored in real-time by an experienced epileptologist (PF). Raw EEG data were stored for offline analyses.

2.3. Intracranial EEG data processing

All EEG data processing was performed using ScanEdit v4.4 (Compumedics NeuroScan). Gradient switching artifact was removed using average artifact subtraction, which uses the regularity of the gradient switching induced waveform to generate a moving average artifact that can be successfully removed from the baseline EEG (Allen et al., 2000). Cardioballistic artifact is commonly seen in routine scalp EEG recordings. It is greatly amplified when EEG is recorded in the MR environment because movement of electrically conductive material in

a static field results in electromagnetic induction. In contrast, cardioballistic artifact is not seen in routine clinical intracranial EEG records, nor was it seen in our intracranial EEG recordings in the MR environment. Therefore, removal of this artifact was not necessary. The reason why this artifact is not seen in clinical intracranial EEG recordings or in our iEEG-fMRI recordings is that intracranial electrodes

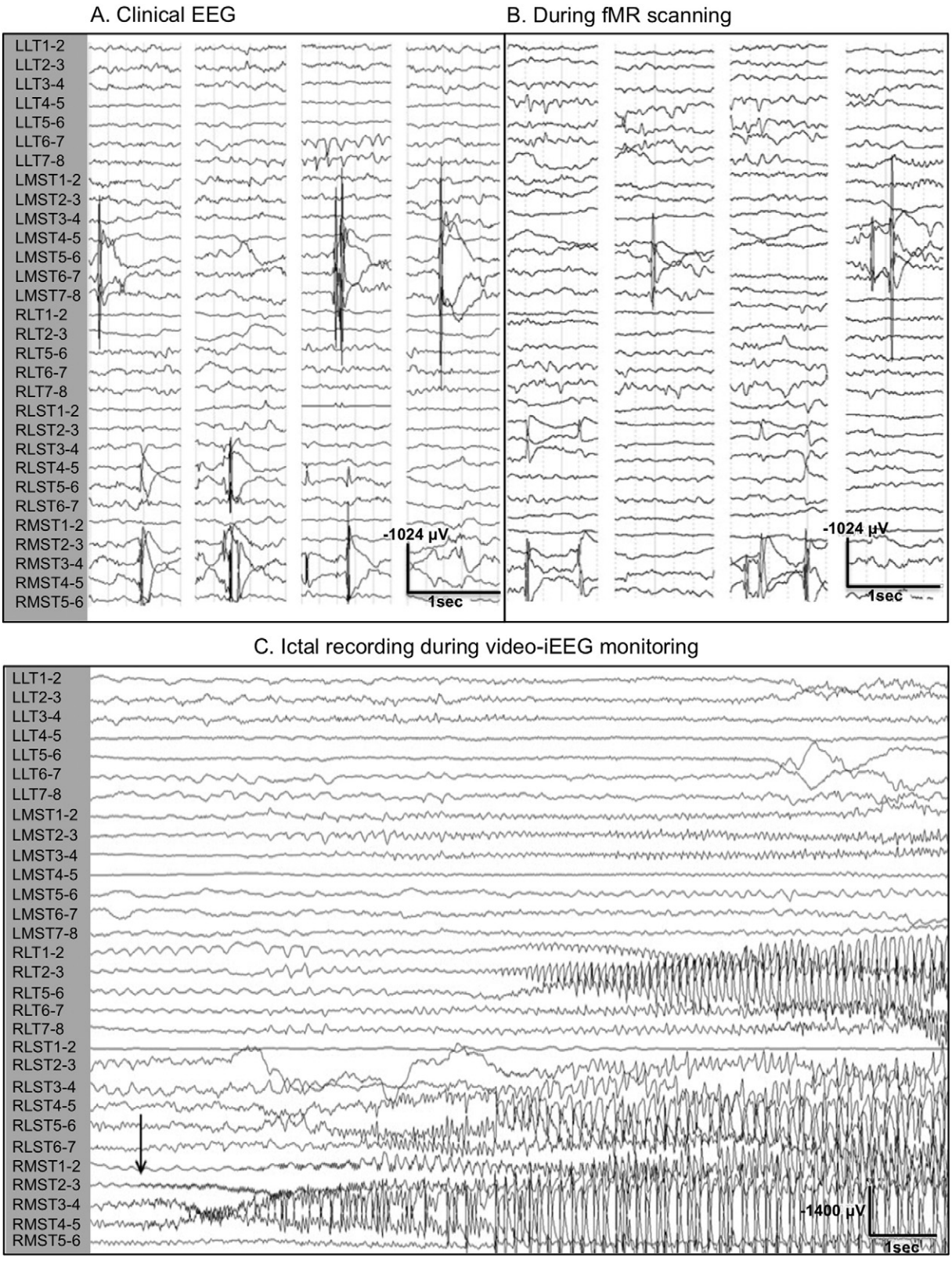

Fig. 1. Intracranial EEG recordings from patient 3. (A) Interictal iEEG recordings obtained in our Seizure Monitoring Unit. (B) Intracranial EEG of clinical quality acquired during simultaneous fMR image acquisition at 3 T. (C) Ictal iEEG recording of a right mesial temporal lobe seizure recorded in our Seizure Monitoring Unit. Note that the EEG samples in A and B are 1 s data segments containing interictal epileptiform discharges.

(depth or subdural electrodes) are less prone to movement with cardiac pulsations because they are fixed to the skull or dura. Additionally, the distance between the active and reference electrodes is smaller for iEEG than scalp EEG, which further reduces the amplitude of cardioballistic artifact.

A low-pass filter at 30 Hz was applied to the EEG data, and a bipolar montage for each electrode bank was generated. Two experienced electroencephalographers (PF, YA) reviewed the EEG data noting the timing, morphology, and location of interictal discharges. Examples of iEEG recorded outside the MR scanner in the seizure monitoring unit for clinical purposes using a clinical EEG recording system (Natus Xltek NeuroWorks, Natus Medical Incorporated, San Carlos, CA) and inside the MR scanner are shown in Fig. 1.

2.4. fMRI data processing

fMRI data processing was carried out using FEAT [FMRI Expert Analysis Tool, Version 6.00, part of FSL (FMRIB's Software Library, http://www.fmrib.ox.ac.uk/fsl)]. The following pre-processing was applied: motion correction using MCFLIRT [Motion Correction: FMRIB's Linear Image Registration Tool (Jenkinson et al., 2002)], slice-timing correction using Fourier-space time-series phase-shifting; non-brain removal using the Brain Extraction Tool (Smith, 2002), spatial smoothing using a Gaussian kernel of FWHM 6.0 mm; high-pass temporal filtering (Gaussian-weighted least-squares straight line fitting, with sigma = 50.0 s). Registration of fMRI data to high-resolution structural and standard-space images was carried out using FLIRT [FMRIB's Linear Image Registration Tool (Jenkinson et al., 2002; Jenkinson and Smith, 2001)]. Because patient movement was minimal (<3 mm) in most patients, motion parameters were not included as regressors since motion correction via MCFLIRT [Motion Correction: FMRIB's Linear Image Registration Tool (Jenkinson et al., 2002)] sufficiently minimized any motion effects.

The binary timing of interictal discharges was convolved with multiple hemodynamic response functions (HRFs) with time-to-peak ranging from 0–13 s, similar to the methodology employed for scalp EEG-fMRI analyses by other groups (Bagshaw et al., 2004; Kobayashi et al., 2006a; Kobayashi et al., 2006b). The generated model was imported into FEAT where a time-series statistical analysis was carried out using FILM (FMRIB's Improved Linear Model) with local autocorrelation correction for each run (Woolrich et al., 2001). Higher-level analyses were performed using a fixed effects model, by forcing the random effects variance to zero in FLAME (FMRIB's Local Analysis of Mixed Effects) (Beckmann et al., 2003; Woolrich et al., 2004; Woolrich, 2008), generating a statistical average of all runs. To account for the increased probability of Type 1 error through the use of multiple HRFs, data were corrected using AlphaSim of the AFNI analysis package http://afni.nimh.nih.gov/pub/dist/doc/program_help/AlphaSim.html that performs both probability and cluster-based thresholding at a significance level of $p < 0.05$, as determined by Monte Carlo simulations (Ward, 2000). Locations of the strongest activation were identified as the cluster (as determined by AlphaSim) with maximum peak response (Z-score). The gamma function time-to-peak for each subject's maximal response was used. Parametric maps were overlaid onto high-resolution structural images that were registered to MNI standard space.

The BOLD response(s) for each IED was visually evaluated. If the BOLD response was within 1 cm of the center of recording electrode(s) showing maximal involvement of the IEDs (defined as the maximal amplitude in referential montage and/or phase reversal in bipolar montage), there was considered to be good concordance between BOLD response and the recorded discharges. A significant BOLD response in the same lobe as the active electrode was assessed as relative concordance, and outside of the same lobe as poor concordance.

3. Results

3.1. Subjects

All twelve patients underwent simultaneous intracranial EEG-fMRI data acquisition without adverse event. Three subjects were excluded from analysis due to inadequate grounding of the EEG signal and persistent MR gradient switching EEG artifact that could not be removed during post-processing, which rendered the EEG uninterpretable. Patient movement during data collection was limited as all patients but one had a maximum displacement <3 mm. One patient had a maximum displacement of 20 mm on a few occasions during scanning. The segments containing >3 mm displacement for this patient were excluded from analysis. Of the nine analyzed datasets, the ictal semiology was suggestive of a temporal focus in 7 patients (one neocortical) and a frontal focus in 2 patients (Table 1). Structural MRI revealed no lesion in 4 patients, but revealed mesial temporal lobe sclerosis in 1, bilateral periventricular nodular heterotopia in 1, enlarged amygdala in 1, unilateral perisylvian polymicrogyria in 1, and unilateral post-traumatic encephalomalacia in frontotemporal region in 1.

3.2. Clinical EEG data

All patients underwent scalp VEM. Generally, the interictal EEG findings were not well localized except for patient 6 who had epileptiform discharges over the left temporal lobe (Table 1). The ictal EEG changes were also poorly localized except for patients 6 and 7, who both had seizure onsets over the left temporal area. All patients except patients 6, 7, and 9 had bilateral electrode implantation using subdural strips with or without depth electrodes. Patient 6 had unilateral grid, strip and depth electrodes, patient 7 had unilateral subdural strip and depth electrodes, and patient 9 had subdural strip electrodes. Subjects had between 48 and 156 recording contacts (mean = 82). Interpretation of the intracranial VEM data identified the seizure onset zone in all subjects: unilateral mesial temporal lobe in 2 patients, independent bilateral temporal lobe in 3, temporal neocortex in 2, and multifocal in 2 (Table 1).

3.3. iEEG-fMRI data

iEEG of clinical quality was recorded during functional MR scanning (Fig. 1B). Based on the location of spiking, 11 different types of IEDs were recorded during iEEG-fMRI studies ranging from 37–2611 discharges per location (mean 857 ± 286). Subjects were divided into the following groups based on the location of the contact where the discharges were most frequently observed: mesial temporal, lateral temporal, and extra-temporal.

3.3.1. Mesial temporal discharges

Seven (5 left, 2 right) mesial temporal IED types were recorded in five patients (patients 1–5; patients 2 and 3 had bilateral independent temporal epileptic foci). The number of discharges recorded in these patients ranged from 110–2092 with an average of 738 ± 353 discharges. Six of the 7 mesial temporal IEDs had a BOLD response with good concordance (<1 cm distance) in the ipsilateral mesial temporal structures with an average Z-score of 5.8 (range 3.15–9.65) and an average activated cluster volume of 3.14 cm^3 (range 0.75–8.61 cm^3, Fig. 2A, Table 2). Four of these discharge types had additional extra-temporal BOLD clusters: contralateral parietal in 2 patients, bilateral frontal–parietal in 2, ipsilateral temporal–parietal in 1, bilateral occipital in 1, contralateral insula in 1, and contralateral temporal pole in 1 (Fig. 2A). The BOLD cluster with the maximum Z-score value was located at the discharge location in 2 datasets (subject 2 right and left), and was extra-temporal in 5 (patients 1, 3, right and left, 4, 5). One subject (subject 5) in this group had a significant BOLD cluster only in the ipsilateral occipital cortex (poor concordance). Notably, this subject showed a large area of electrode susceptibility artifact over the temporal lobe that was likely worsened by additional movement artifact. This, in turn, resulted in

Table 1
Demographic, ictal semiology, MRI and EEG data of the study subjects.

Pt	Age/sex	Seizure semiology	MRI findings	Scalp EEG interictal	Scalp EEG ictal onset	iEEG coverage	iEEG interictal	iEEG ictal onset	Surgery	Outcome, F/U
1	20/♀	Abdominal pain → Hyperventilation → Staring→ LOC and oral automatism → 2° GTC	Bil PVNH L > R	Bil FT	1. RFT 2. LT	R:Am, Hc, PVNH L: mesial & lateral F, and sub T	Active LT, rare R mesial T	L T	LT lobectomy	Class I, 5 yrs
2	29/♀	1. Smell→ Flashing light→ Deja vu → LOC 2. Nocturnal GTC	L enlarged Am	Bil T	Bil T	R: lateral, mesial & sub T L: lateral, mesial & sub T	Bil mesial T	Bil TLE	Bil HS	Class IV, 5 yrs
3	52/♀	1. Deja vu→ Smell → LOC 2. Nocturnal GTC	Normal	Bil T, R > L	Bi T	R: mesial, lateral, & sub T L: mesial, lateral, & sub T	Bil TR > L	Bil TLE	Not operated	Class III, 9 mo
4	24/♂	Gustatory, epigastric, flashing Light staring → with LOC, oral and arm automatisms → 2° GTC	Normal	Bil F, R > L (rare)	Bi T	R: mesial, inferior & lateral T–O L: mesial, inferior & lateral T–O	Bil mesial T	Bil TLE	Not operated	Seizure free, 2 yrs
5	56/♀	Head turning to L → R arm stiffening → 2° GTC	L MTS	Bil T, L > R	1. LF 2. Bil F 3. Diffuse	R: mesial — sub T, lateral FT, & lateral F Lateral F L: mesial — sub T, lateral FT, & lateral F Lateral F	Multifocal: LT, RT LF, RF	L mesial T	LT neocortex[a]	Class IV, 6 mo
6	27/♀	Deja vu, chest /abdominal discomfort → Staring with LOC and R eye blinking and nocturnal GTC	L perisylvian PMG	LT	LT	L: orbito F and T, lateral F & inslua Insula	L anterior T	L anterior T	LT lobectomy	Class I, 3 yrs
7	24/♀	Hears music → Loss of speech → At times 2° GTC	LF-T Encephalomalacia	None	LT	L: lateral T, anterior T, Hc, first T gyrus, & Heschl gyrus	LT neocortex	LT neocortex	LT neocortex[a]	Class I, 1 yr
8	29/♀	1. Staring with LOC and gibberish speech 2. Head turning to R then GTC	Normal	GSW max F	GSW max L F	R: lateral, mesial & orbito F L: lateral, mesial & sub F	Multifocal: LF, RF	Multifocal: LF, RF	Not operated	Seizure free, 4 mo
9	22/♂	Headache, dreamy state, loss of speech → LOC with oral automatism → 2° GTC	Normal	LT, LP—post T	LP-O-post T	L: lateral O, T, P, and under O & T	Multifocal: P, T, O	Multifocal: P, T, O	Not operated	Unchanged, 1 yr

Abbreviations: Am amygdala, Bil bilateral, F frontal, FT frontotemporal, GTC generalized tonic–clonic seizures, GSW generalized spike/polyspike and wave, Hc hippocampus, HS hippocampal stimulator, I insula, L left, LOC loss of consciousness, mo month, max maximal, MTS mesial temporal sclerosis, NA not available, O occipital, P parietal, PMG polymicrogyria, PVNH periventricular nodular heterotopia, R right, T temporal, yr year.
[a] Sparing mesial T structures.

significant loss of BOLD signal in the temporal region (Fig. 2A, Table 2). Patient 1, with good concordance, underwent left temporal lobectomy with class I outcome, and patient 5, with poor concordance, had a large left temporal neocortical resection with class IV outcome. Patients 2, 3, and 4 did not undergo surgical resection.

3.3.2. Temporal neocortical discharges

Two subjects had left temporal neocortical discharges. Patient 6 had concordant BOLD activation in the ipsilateral posterior hippocampus, ipsilateral frontal and posterior temporal lobe, and contralateral insula (good concordance, Fig. 2B). Patient 7 had multifocal BOLD clusters in the ipsilateral frontal opercular, frontoparietal, parieto-occipital, post-temporal–occipital cortices, and cerebellum in the other (relative concordance, Fig. 2B). Both achieved class I outcome with left temporal lobectomy and left temporal neocortical resection, respectively.

3.3.3. Extratemporal discharges

These two subjects (patients 8 and 9) with left posterolateral frontal and left parietal discharges showed no BOLD response at the location of the interictal discharges (Fig. 2C). Subject 8 showed a BOLD response in the ipsilateral orbitofrontal, contralateral frontal and contralateral temporal pole (relative concordance). For subject 9, a BOLD response was seen in the bilateral parietal cortices with maximum *Z*-score in the contralateral parietal region (poor concordance). These patients did not undergo surgical resection due to poor clinical iEEG localization of the seizure focus.

Table 2
iEEG and BOLD response data of the 11 iEEG epileptiform discharge types recorded during fMR scanning.

Pt	Number of IEDs	Location of IEDs	BOLD at location of spike	Max *Z* score at location of spike	Volume of BOLD at location of spike (cm^3)	Distance from susceptibility (mm)	BOLD in other location(s)	Location of max BOLD	Max *Z* score	Volume of max BOLD (cm^2)	Time to peak BOLD (sec)	Max patient movement (mm)
1	216	L parahippocampus	Yes	3.68	5.84	12	R mesial P	R mesial P	3.68	0.71	5	0.6
2a	184	R mesial T	Yes	6.14	8.61	8	No	R mesial T	6.14	8.61	4.5	2.0
2b	277	L mesial T	Yes	5.31	1.14	12	No	L mesial T	5.31	1.14	5	2.0
3a	2035	R mesial T	Yes	4.43	0.75	14	Bil F—P, R mesial T-P, LT pole	R mesial P	9.65	532.50	7	2.0
3b	253	L mesial T	Yes	3.15	0.91	14	Bil Occipital, RP, R insula	R cuneous	4.98	68.21	8	2.0
4	2092	L mesial T	Yes	5.94	1.57	14	Bil post F—P	LP-O	6.78	256.25	5.5	1.5
5	110	L mesial T	No	–	–	12	LO	LO	3.2	0.86	8	20
6	1541	L lateral T	Yes	5.77	10.26	26	L post Hc	L lateral T	5.77	10.26	4	1.2
7	75	L middle T gyrus	No	–	–	12	LF opercular, L post F—P, LP-O, L post T-O, L cerebellum	LF operculum	4.4	2.78	7	1.3
8	37	L posterolateral F	No	–	–	20	L orbito-F, RF, RT pole	RF	3.19	1.14	8	1.3
9	2611	L anterior P	No	–	–	44	LP, RP	RP	4.73	1.04	4.5	1.5

Abbreviations: Bil bilateral, F frontal, Hc hippocampus, IED interictal epileptiform discharge, L left, O occipital, P parietal, R right, T temporal.

4. Discussion

This study has produced several notable findings about BOLD signal changes associated with focal IEDs recorded by intracranial electrodes. First, our data confirm the results of our and other studies of the feasibility and low-risk of iEEG-fMRI when performed under controlled conditions (Boucousis et al., 2012; Carmichael et al., 2012; Cunningham et al., 2012; Vulliemoz et al., 2011).

Second, significant BOLD activation was seen in all 9 (out of a total of 12) patients in whom interpretable EEG was obtained. Previous scalp EEG-fMRI studies detected BOLD responses associated with IEDs in 50–60% and 60–70% of patients studied with spike-triggered or continuous EEG-fMRI, respectively (Mulert and Lemieux, 2009). Other research groups have shown that the yield of scalp EEG-fMRI can be increased to 80–100% by performing convolutions using multiple hemodynamic response functions peaking at 3, 5, 7, and 9 s (Kobayashi et al., 2006a; Kobayashi et al., 2006b; Pittau et al., 2012). Following the success of this analytical approach, we employed a multiple HRF model for our analyses that may in part, explain the high yield from the present study. Another possible explanation may be the high number of epileptiform discharges that were analyzed in our subjects (range 37–2611, mean 857 ± 286). The nature of intracranial EEG also offers the advantage of recording of epileptiform activity without attenuation by the dura, skull, and scalp, which has been theorized to act as a physiological signal filter that allows only the IEDs of the greatest amplitude, which recruit large areas of the cortex, to be visible on scalp EEG (Tao et al., 2005). Additionally, seemingly spike-free periods seen on scalp EEG-fMRI may have IEDs that cannot be detected by scalp EEG. The presence of these unrecorded discharges could contaminate the baseline BOLD signal used for statistical comparison to the periods of spiking by the fMRI general linear model (GLM). Intracranial EEG-fMRI circumvents this limitation; however, it offers limited sampling of the brain that is dependent on the placement of intracranial EEG electrodes. Three EEG datasets, performed early in this project, were deemed uninterpretable due to persistent artifact, attributed to insufficient grounding of the EEG signal by the 20-electrode connector, and a lack of synchronization between the internal clocks of the MRI and EEG systems. We have experienced no further losses of data (2011 to present) since subsequently using a new 64-electrode connector and an MRI-to-EEG clock synchronizer (Compumedics NeuroScan).

Third, we found high concordance between location of the recorded IEDs and BOLD responses. The highest concordance was seen with mesial temporal lobe epileptiform discharges, with 6 of the 7 patients (86%) showing good concordance. The remaining patient (subject 5) with mesial temporal discharges had an ipsilateral occipital BOLD response without any temporal BOLD signal. Interestingly, this patient had a poor postsurgical outcome. It would therefore be tempting to speculate that the lack of a significant BOLD response in the intended surgical target should prompt a search for an ictal onset zone elsewhere in the brain, particularly where the BOLD response was seen, which in this case, was not covered by intracranial EEG electrodes. However, the poor concordance in this case may also be partly related to significant BOLD signal loss in the temporal region due to susceptibility artifact resulting from a combination of a high number of temporal electrodes and a large amount of patient motion (>20 mm) during the scanning session limiting the amount of analyzable data collected.

The higher likelihood of good concordance in the mesial temporal group seen in the present study compared to previous studies looking at iEEG and scalp EEG-fMRI data separately (Al-Asmi et al., 2003; Benar et al., 2006; Lazeyras et al., 2000), may be related to our capability of iEEG to record IEDs for fMRI correlation with higher spatial resolution and sensitivity than scalp EEG. Furthermore, the criteria used to measure concordance in the present study, <1.0 cm between the IED and BOLD response location, is stricter than previously published work that used <2.0 cm between area of interest (resection margin) and BOLD response as selection for good concordance (An et al., 2013).

Good concordance was seen in one of two patients with neocortical discharges and relative concordance in the other. In the two subjects with extra-temporal epileptiform discharges, one in the left frontal lobe and the other in the left parietal lobe, significant BOLD responses were seen in the same lobe, but not adjacent to the recording electrodes.

The small number of patients with lateral temporal and extra-temporal spikes is one limitation of our study that precludes definitive conclusions about these groups. However a trend towards a possible difference in the degree of concordance between the lateral and extra-temporal groups compared to the mesial temporal group was seen.

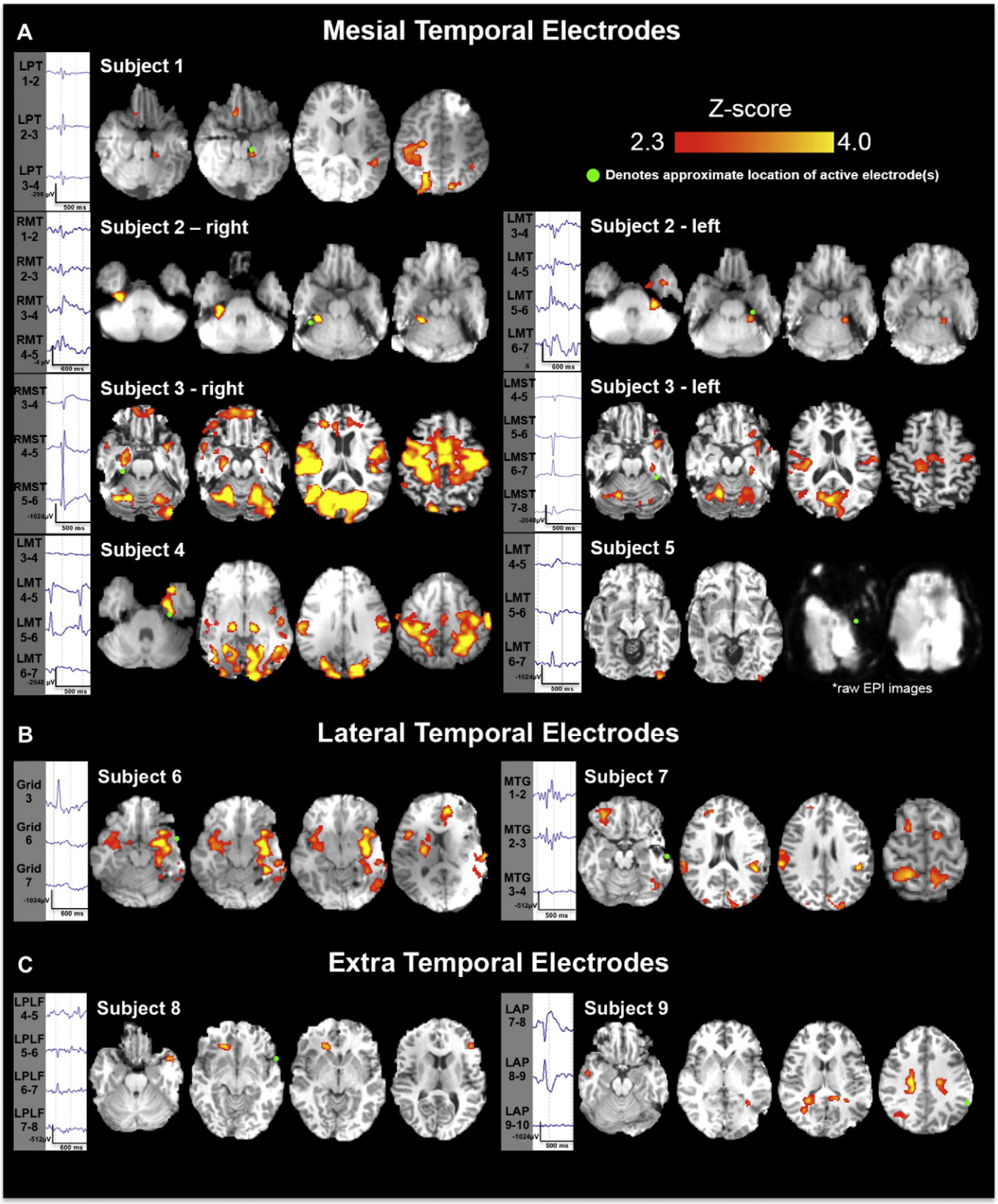

Fig. 2. Significant BOLD clusters associated with interictal discharges recorded via simultaneous iEEG-fMRI. (A) Mesial temporal lobe patients. Significant BOLD clusters ($p < 0.05$, AlphaSim correction) were found in all 5 subjects in this group. Two patients had independent, bilateral temporal discharges that were modeled independently of one another providing 7 datasets for analysis. A significant cluster is found adjacent to the active intracranial electrode contact (marked by a green circle) in 6/7 analyses. One patient (subject 5), had a large amount of susceptibility artifact in the left temporal lobe associated with a large amount of subject motion during data collection. (B) Lateral temporal lobe patients. Significant BOLD clusters ($p < 0.05$, AlphaSim correction) were found in both patients in this group. A significant cluster was found adjacent to the active intracranial electrode contact (green circle) in 1 of 2 analyses. (C) Extratemporal patients. Two patients with extra-temporal lobe epilepsy showed no significant clusters adjacent to the active electrode(s).

This could be due to a difference in the functional character of IEDs from mesial temporal sources versus neocortical temporal and extratemporal discharges (Laufs and Duncan, 2007). The lack of concordance in the extra temporal patients may also highlight an inability to fully localize the ictal onset zone using clinical data (iEEG VEM, MR, positron emission tomography, single photon emission computerized tomography, etc.) as can occur in focal cortical dysplasia, for example (Cendes, 2013). Indeed, it is possible that the intracranial EEG electrodes were not placed at the center of the irritative zone, but instead were placed at the edge. Thus, the site of maximum BOLD activation seen in these subjects may in fact be the center of the irritative zone, where electrodes were not placed, and possibly, should have been placed. Consistent with our findings, the subjects with extratemporal IEDs were not offered surgery since ictal iEEG recordings failed to identify the seizure onset zone. As previous work has shown, scalp EEG-fMRI may sometimes provide additional data to direct subsequent clinical investigations that can improve patient post-surgical outcomes (Zijlmans et al., 2007). We feel that iEEG-fMRI may have a similar function.

Overall, significant BOLD responses were seen distant from the active electrode in 9 of 11 (82%) datasets (Table 2). In fact, the cluster with maximum BOLD response was found to be distant rather than adjacent to the active electrode in 8 out of 11 datasets (contralateral in 3). We hypothesize that this may be a result of EPI signal loss due to the susceptibility artifact associated with the intracranial electrodes. Indeed, as discussed in our previous work detailing the susceptibility artifact associated with iEEG-fMRI (Boucousis et al., 2012), T2* signal intensity can be decreased up to 40% within 1.5 cm of the intracranial electrode; at a distance 2.0 cm from the electrode, signal loss is negligible. This decrease in signal-to-noise ratio may have negatively impacted the statistical analyses performed on these data (Parrish et al., 2000), leading to an underestimation of the strength of activation immediately adjacent to the site of the active intracranial electrode contact.

Extra-temporal BOLD clusters generated from temporal spikes have been previously reported in a scalp EEG-fMRI study of 35 patients with lesional and non-lesional mesial and neocortical temporal lobe epilepsy (Kobayashi et al., 2006a). Unilateral temporal discharges (mesial and neocortical) were associated with BOLD activation in ipsilateral mesial temporal structures, ipsilateral basal ganglia, bilateral neocortical temporal regions and in the contralateral temporal lobe. The observed patterns of BOLD activation did not show a correlation with the location of the discharges or with the presence or absence of a lesion. Comparison of this study to ours is challenging, especially for our mesial temporal subjects, since strictly mesial temporal discharges cannot be recorded on scalp EEG; instead, these discharges reflect simultaneous involvement of the mesial and neocortical temporal lobes. Despite this, we observed similar widespread patterns of BOLD activation involving mesial and neocortical temporal and extra-temporal sites. The small number of patients in our study, combined with patient heterogeneity does not allow any conclusions or associations to be made between the underlying lesion type or location of discharge with the pattern of BOLD activation. One notable exception, however, was subject 2, who had non-lesional independent bitemporal lobe seizures and independent mesial temporal lobe discharges. This subject, unlike all the other patients in our study, had very focal BOLD signal increases that were maximal and adjacent to the active electrode. The reasons for this unique pattern of BOLD activation are unclear as there appear to be no clear clinical, EEG, or MR imaging characteristics that differentiate this subject from the others in our study.

The functional connectivity of the temporal lobe to other cortical and subcortical structures, and the rapid propagation of spikes may explain the extra-temporal BOLD responses from temporal lobe spikes seen in previous studies (Kobayashi et al., 2006a; Walker et al., 2010) and our study. This may also apply to extra-temporal epileptiform discharges, explaining the BOLD responses in distant areas. In our study, 3 patients had a maximum BOLD response near the location of the active electrode. In the remaining, the maximum BOLD response was distant to the active electrode even though a significant BOLD response was seen at the active electrode. This might suggest that the spike generator is distant from the active electrode. However, we feel that this is not the case for several reasons: First, the limited intracranial electrode recording field makes it very unlikely that recorded spikes originated from a distant active electrode. Second, clinical recordings of seizures confirmed that the ictal onset zone included the active electrodes used in our iEEG-fMRI analyses (Fig. 1C). Furthermore, three of our subjects had resections that included the active electrode contact and they are now seizure-free. Lastly, susceptibility artifact is present in the immediate vicinity of intracranial EEG electrodes (Table 2) which results in attenuation of the BOLD signal in up to 20 mm of cortex adjacent to the active electrode(s) (Boucousis et al., 2012; Cunningham et al., 2012). This may explain the lack of a maximum BOLD response immediately adjacent to the active electrode contact.

Despite the limitation of signal loss near the electrodes, intracranial EEG-fMRI offers a number of advantages over scalp EEG-fMRI and other imaging methods. These include the ability to study very focal or low amplitude epileptiform discharges not recordable by scalp EEG (e.g., IEDs that do not require >10 cm^2 of cortical surface activity) or discharges originating from deep structures such as mesial temporal structures or the cingulate gyrus. More importantly, iEEG-fMRI opens a new avenue for a better understanding of the hemodynamic response to epileptiform discharges by affording the opportunity to study very focal discharges with great precision or for further mapping the seizure network by providing information that could be complementary to routine clinical investigations such as EEG, structural MRI, PET, and SPECT (An et al., 2013; Gotman and Pittau, 2011; Laufs and Duncan, 2007; Moeller et al., 2009; Thornton et al., 2010; Zijlmans et al., 2007). Although ictal EEG and high frequency oscillations are better markers of the epileptogenic zone than IEDs, IEDs still provide useful clinical information about the irritative zone, which often includes the ictal onset zone. Therefore, iEEG-fMRI may provide a better understanding of the irritative zone and consequently the ictal onset zone because it can delineate the irritative zone with greater spatial resolution than iEEG alone, which provides limited sampling of the brain. Lastly, intracranial EEG-fMRI may allow the study of the hemodynamic response to high frequency oscillations.

5. Conclusions

iEEG-fMRI is a feasible and low-risk method for assessment of the hemodynamic changes associated with very focal interictal epileptiform discharges that cannot typically be recorded using scalp EEG-fMRI. We also demonstrated high yield and concordance rates of BOLD responses to interictal epileptiform discharges of mesial temporal discharges. Notably, however, most datasets (8/11) showed maximal BOLD signal at locations distant to the most active electrode contact. Intracranial EEG-fMRI may provide useful data to help better understand the functional networks generating interictal discharges in focal epilepsy.

Acknowledgments

This work was supported by the Canadian Institutes for Health Research (MOP-136839). CB was supported by a Clinician Researcher Training award from Alberta Innovates — Health Solutions.

References

Al-Asmi, A., Bénar, C.G., Gross, D.W., Khani, Y.A., Andermann, F., Pike, B., Dubeau, F., Gotman, J., 2003. fMRI activation in continuous and spike-triggered EEG-fMRI studies of epileptic spikes. Epilepsia 44 (10), 1328–1339. http://dx.doi.org/10.1046/j.1528-1157.2003.01003.x14510827.

Allen, P.J., Josephs, O., Turner, R., 2000. A method for removing imaging artifact from continuous EEG recorded during functional MRI. Neuroimage 12 (2), 230–239. http://dx.doi.org/10.1006/nimg.2000.059910913328.

An, D., Fahoum, F., Hall, J., Olivier, A., Gotman, J., Dubeau, F., 2013. Electroencephalography/functional magnetic resonance imaging responses help predict surgical outcome

in focal epilepsy. Epilepsia 54 (12), 2184–2194. http://dx.doi.org/10.1111/epi.1243424304438.
Bagshaw, A.P., Aghakhani, Y., Bénar, C.G., Kobayashi, E., Hawco, C., Dubeau, F., Pike, G.B., Gotman, J., 2004. EEG-fMRI of focal epileptic spikes: analysis with multiple haemodynamic functions and comparison with gadolinium-enhanced MR angiograms. Hum. Brain Mapp. 22 (3), 179–192. http://dx.doi.org/10.1002/hbm.2002415195285.
Beckmann, C.F., Jenkinson, M., Smith, S.M., 2003. General multilevel linear modeling for group analysis in FMRI. Neuroimage 20 (2), 1052–1063. http://dx.doi.org/10.1016/S1053-8119(03)00435-X14568475.
Bénar, C.G., Grova, C., Kobayashi, E., Bagshaw, A.P., Aghakhani, Y., Dubeau, F., Gotman, J., 2006. EEG-fMRI of epileptic spikes: concordance with EEG source localization and intracranial EEG. Neuroimage 30 (4), 1161–1170. http://dx.doi.org/10.1016/j.neuroimage.2005.11.00816413798.
Boucousis, S.M., Beers, C.A., Cunningham, C.J., Gaxiola-Valdez, I., Pittman, D.J., Goodyear, B.G., Federico, P., 2012. Feasibility of an intracranial EEG-fMRI protocol at 3 T: risk assessment and image quality. Neuroimage 63 (3), 1237–1248. http://dx.doi.org/10.1016/j.neuroimage.2012.08.00822902923.
Carmichael, D.W., Vulliemoz, S., Rodionov, R., Thornton, J.S., McEvoy, A.W., Lemieux, L., 2012. Simultaneous intracranial EEG-fMRI in humans: protocol considerations and data quality. Neuroimage 63 (1), 301–309. http://dx.doi.org/10.1016/j.neuroimage.2012.05.05622652020.
Cendes F., Neuroimaging in investigation of patients with epilepsy. Continuum (Minneap Minn), 19(3 Epilepsy) (2013) 623–642 [doi:10.1212/01.CON.0000431379.29065.d3] [Pubmed: 23739101]
Cunningham, C.B., Goodyear, B.G., Badawy, R., Zaamout, F., Pittman, D.J., Beers, C.A., Federico, P., 2012. Intracranial EEG-fMRI analysis of focal epileptiform discharges in humans. Epilepsia 53 (9), 1636–1648. http://dx.doi.org/10.1111/j.1528-1167.2012.03601.x22881457.
Ferree, T.C., Clay, M.T., Tucker, D.M., 2001. The spatial resolution of scalp EEG. Neurocomputing 38–40, 1209–1216. http://dx.doi.org/10.1016/S0925-2312(01)00568-9.
Gotman, J., Pittau, F., 2011. Combining EEG and fMRI in the study of epileptic discharges. Epilepsia 52 (Suppl. 4), 38–42. http://dx.doi.org/10.1111/j.1528-1167.2011.03151.x21732941.
Jenkinson, M., Bannister, P., Brady, M., Smith, S., 2002. Improved optimization for the robust and accurate linear registration and motion correction of brain images. Neuroimage 17 (2), 825–841. http://dx.doi.org/10.1006/nimg.2002.113212377157.
Jenkinson, M., Smith, S., 2001. A global optimisation method for robust affine registration of brain images. Med. Image Anal. 5 (2), 143–156. http://dx.doi.org/10.1016/S1361-8415(01)00036-611516708.
Kobayashi, E., Bagshaw, A.P., Bénar, C.G., Aghakhani, Y., Andermann, F., Dubeau, F., Gotman, J., 2006a. Temporal and extratemporal BOLD responses to temporal lobe interictal spikes. Epilepsia 47 (2), 343–354. http://dx.doi.org/10.1111/j.1528-1167.2006.00427.x16499759.
Kobayashi, E., Bagshaw, A.P., Grova, C., Dubeau, F., Gotman, J., 2006b. Negative BOLD responses to epileptic spikes. Hum. Brain Mapp. 27 (6), 488–497. http://dx.doi.org/10.1002/hbm.2019316180210.
Lachaux, J.P., Rudrauf, D., Kahane, P., 2003. Intracranial EEG and human brain mapping. J. Physiol. Paris 97 (4–6), 613–628. http://dx.doi.org/10.1016/j.jphysparis.2004.01.01815242670.
Laufs, H., Duncan, J.S., 2007. Electroencephalography/functional MRI in human epilepsy: what it currently can and cannot do. Curr. Opin. Neurol. 20 (4), 417–423. http://dx.doi.org/10.1097/WCO.0b013e3282202b9217620876.
Lazeyras, F., Blanke, O., Perrig, S., Zimine, I., Golay, X., Delavelle, J., Michel, C.M., de Tribolet, N., Villemure, J.G., Seeck, M., 2000. EEG-triggered functional MRI in patients with pharmacoresistant epilepsy. J. Magn. Reson. Imaging 12 (1), 177–185. http://dx.doi.org/10.1002/1522-2586(200007)12:1<177::AID-JMRI20>3.0.CO;2-310931578.
Moeller, F., Tyvaert, L., Nguyen, D.K., LeVan, P., Bouthillier, A., Kobayashi, E., Tampieri, D., Dubeau, F., Gotman, J., 2009. EEG-fMRI: adding to standard evaluations of patients with nonlesional frontal lobe epilepsy. Neurology 73 (23), 2023–2030. http://dx.doi.org/10.1212/WNL.0b013e3181c55d1719996077.
Morris 3rd, H.H., Lüders, H., 1985. Electrodes. Electroencephalogr. Clin. Neurophysiol. Suppl. 37, 3–263859406.
Mulert, C., Lemieux, L., 2009. EEG-fMRI: Physiological Basis, Technique, and Applications. Springer.
Parrish, T.B., Gitelman, D.R., LaBar, K.S., Mesulam, M.M., 2000. Impact of signal-to-noise on functional MRI. Magn. Reson. Med. 44 (6), 925–932. http://dx.doi.org/10.1002/1522-2594(200012)44:6<925::AID-MRM14>3.0.CO;2-M11108630.
Pittau, F., Dubeau, F., Gotman, J., 2012. Contribution of EEG/fMRI to the definition of the epileptic focus. Neurology 78 (19), 1479–1487. http://dx.doi.org/10.1212/WNL.0b013e3182553bf722539574.
Smith, S.M., 2002. Fast robust automated brain extraction. Hum. Brain Mapp. 17 (3), 143–155. http://dx.doi.org/10.1002/hbm.1006212391568.
Tao, J.X., Ray, A., Hawes-Ebersole, S., Ebersole, J.S., 2005. Intracranial EEG substrates of scalp EEG interictal spikes. Epilepsia 46 (5), 669–676. http://dx.doi.org/10.1111/j.1528-1167.2005.11404.x15857432.
Thornton, R., Laufs, H., Rodionov, R., Cannadathu, S., Carmichael, D.W., Vulliemoz, S., Salek-Haddadi, A., McEvoy, A.W., Smith, S.M., Lhatoo, S., Elwes, R.D., Guye, M., Walker, M.C., Lemieux, L., Duncan, J.S., 2010. EEG correlated functional MRI and post-operative outcome in focal epilepsy. J. Neurol. Neurosurg. Psychiatry 81 (8), 922–927. http://dx.doi.org/10.1136/jnnp.2009.19625320547617.
Vulliemoz, S., Carmichael, D.W., Rosenkranz, K., Diehl, B., Rodionov, R., Walker, M.C., McEvoy, A.W., Lemieux, L., 2011. Simultaneous intracranial EEG and fMRI of interictal epileptic discharges in humans. Neuroimage 54 (1), 182–190. http://dx.doi.org/10.1016/j.neuroimage.2010.08.00420708083.
Walker, M., Chaudhary, U., Lemieux, L., 2010. EEG-fMRI in adults with focal epilepsy. In: Mulert, C., Lemieux, L. (Eds.), EEG-fMRI. Springer, Berlin Heidelberg, pp. 309–331.
Ward, B.D., 2000. Simultaneous Inference for fMRI Data. AFNI 3dDeconvolve Documentation, Medical College of Wisconsin.
Woolrich, M., 2008. Robust group analysis using outlier inference. Neuroimage 41 (2), 286–301. http://dx.doi.org/10.1016/j.neuroimage.2008.02.04218407525.
Woolrich, M.W., Behrens, T.E., Beckmann, C.F., Jenkinson, M., Smith, S.M., 2004. Multilevel linear modelling for FMRI group analysis using Bayesian inference. Neuroimage 21 (4), 1732–1747. http://dx.doi.org/10.1016/j.neuroimage.2003.12.02315050594.
Woolrich, M.W., Ripley, B.D., Brady, M., Smith, S.M., 2001. Temporal autocorrelation in univariate linear modeling of FMRI data. Neuroimage 14 (6), 1370–1386. http://dx.doi.org/10.1006/nimg.2001.093111707093.
Zijlmans, M., Huiskamp, G., Hersevoort, M., Seppenwoolde, J.H., van Huffelen, A.C., Leijten, F.S., 2007. EEG-fMRI in the preoperative work-up for epilepsy surgery. Brain 130 (9), 2343–2353. http://dx.doi.org/10.1093/brain/awm14117586868.